Eur. Phys. J. D **19**, 65–72 (2002)
DOI: 10.1140/epjd/e20020056

THE EUROPEAN PHYSICAL JOURNAL D
EDP Sciences

An analytic collisional-radiative model incorporating non-LTE and optical depth effects

J.A. Pomarico[a], D.I. Iriarte, and H.O. Di Rocco[b]

Instituto de Física Arroyo Seco (IFAS), Universidad Nacional del Centro Pinto 399, B7000GHG, Tandil and CONICET, Argentina

Received 12 June 2001 and Received in final form 24 October 2001

Abstract. In this paper we analyze the variations in line intensities ratios due to a non-equilibrium situation and to optical depth effects. A four level model is proposed and the two particular situations for the possible transitions are considered. Electron density and temperature as well as the source thickness are used as independent parameters to find out in which way and extent they modify the ratios of levels populations compared with the ideal case of an equilibrium state and optically thin source. Accordingly with the ion of interest, electron temperatures ranging from $I/20$ to $I/7$ eV (I being the ionization energy), whereas electron densities in the interval from 10^{14} to 10^{20} cm^{-3} will be considered. These ranges are of special interest for diverse applications such as LIBS and measurement of transition probabilities. Some results are presented for real ions and a new expression for the escape factor is also proposed for general plasma conditions.

PACS. 52.25.-b Plasma properties – 52.50.-b Plasma production and heating – 52.70.-m Plasma diagnostic techniques and instrumentation

1 Introduction

Populations distribution and radiation transport are two fundamental aspects to be considered in the description and interpretation of the radiation emitted from spectral sources. These questions arise and are of crucial importance in many branches of plasma physics, including, for example, plasma spectroscopy [1,2], stellar atmospheres [3], the measurement of atomic parameters, such as transition probabilities and rates, laser physics, etc. Because of the high degree of complexity of this problem, it becomes clear that numerical models are to be used involving a limited number of both, system levels and ions present in the plasma. These questions have been addressed by many authors and numerous works have been published giving answers to particular problems from which no always other cases of interest can be inferred. Numerical methods to solve radiation trapping problems include Monte Carlo simulations [4], the piecewise constant approximation [5], and the propagator function method [6]. Newer works, [7–9] include other numerical methods. On the other hand, concerning with the population of energy levels, it is investigated using different approaches and sophisticated codes for atomic calculations [10]. There is no doubt about the validity and importance of these works but, a simple model containing the necessary physics and which can be used reliably is sometimes mandatory. This is of particular interest when using Laser Induced Breakdown Spectroscopy (LIBS) [11], where the spectroscopic data need to be rapidly evaluated for the determination of pollutants and traces.

The main problem, to be addressed in the present work, can be stated in the following terms: given the electron temperature and density, how much does the quotient between the intensities of two lines departures from the simple formula given for both, Local Thermodynamic Equilibrium (LTE) and a thin source? In this particular case, the intensities ratio for two lines $p \to o$, $v \to u$ is given by:

$$R^I_{\mathrm{eq}} = \frac{I_{po}}{I_{vu}} = \frac{I^{\mathrm{Peak}}_{po}\Gamma_{po}}{I^{\mathrm{Peak}}_{vu}\Gamma_{vu}} = \frac{g_p f_{po}\omega^3_{po}}{g_v f_{vu}\omega^3_{vu}} \exp(\beta_{vp}), \qquad (1)$$

where g is the level multiplicity, f is the emission oscillator strength, ω is the emission frequency and the exponent β_{vp} is defined as $\beta_{vp} = (E_v - E_p)/\Theta$, being Θ is the electron temperature measured in energy units. In the above equation, the line widths are designated by Γ and the peak intensities by I^{Peak}.

In a previous work [12], a simple (two levels) model was described considering both, collisional (excitation and deexcitation) and radiative processes. In that work the populations ratio was shown to differ from its LTE expression by a simple factor, designated as $\alpha \equiv \alpha(N_{\mathrm{e}}, T)$, which is a function of the electron density (N_{e}) and the absolute

[a] e-mail: juanp@exa.unicen.edu.ar
[b] e-mail: hdirocco@exa.unicen.edu.ar

temperature (T). By using standard notation [13], and labeling the levels with the indexes v, u such that $E_v > E_u$ it results:

$$\frac{N_v}{N_u} = \left(\frac{g_v}{g_u}\right)\frac{\mathrm{e}^{-\beta_{vu}}}{\alpha_{vu}}, \tag{2}$$

where $\alpha_{vu} \equiv 1 + A_v/N_\mathrm{e}\mathcal{D}_{vu}$. In this last expression, $A_v = \sum_n A_{vn}$, is the total probability of radiative decay from level $|v\rangle$ and $\mathcal{D}_{vu}$ is its de-excitation rate to level $|u\rangle$. In this way, an exact, analytical result was obtained such that, without the need of introducing the escape factor (see Sect. 5), the intensities ratio between two lines I_{po}/I_{vu} is proportional to f_{po}/f_{vu} for a thin source and to $\omega^3_{po}/\omega^3_{vu}$ for thick sources (black body limit).

Note that, in principle, the comparison between population ratios obtained by numerical solution of rate equations (when available) and simple Boltzmann calculations permits to assign a numerical value to the coefficient α_{vu} defined in equation (2). However, its explicit dependence on N_e and T is obscured by the numerical nature of this approach. In the present work we propose analytical expressions for the α's in terms of rate coefficients. Moreover, a generalization of those previous results published in [12] will be presented. Two main aspects will be considered: (i) the system will consist of four levels: the fundamental one, two excited levels, and the ionization limit and (ii) all processes which can induce transitions from or to a given level will be taken into account.

To this end, this work is divided as follows: first we demonstrate that, if the populations ratio can be expressed in the form of equation (2), then the ratio between peak intensities of the lines is given in terms of a function of the electron density and temperature. Next, the new expressions for the α's coefficients of our model are derived for two cases of interest and finally some results are graphically shown.

2 General expressions for the line intensities

Let us consider four arbitrary levels, $|p\rangle$, $|o\rangle$, $|v\rangle$ and $|u\rangle$, and two lines, $p \to o$ and $v \to u$ with intensities denoted by I_{po} and I_{vu}, respectively. We assume that $E_p > E_o$ and $E_v > E_u$ always but there are no restrictions between the states p and v nor between o and u. For a fixed plasma length, L, the integrated intensity is given by the area under the curve [14]

$$I_{po}(\omega) = C_1 \frac{\omega^3_{po}\left[1 - \exp\left(-\kappa_{op}L\right)\right]}{\left[\frac{g_p N_o}{g_o N_p} - 1\right]}, \tag{3}$$

being ω_{po} the frequency of the line, g_p and g_o the multiplicities and N_p and N_o the populations of levels $|p\rangle$ and $|o\rangle$, respectively. In equation (3) κ_{op} is the absorption coefficient, defined by:

$$\kappa_{op} = C_2 f_{op} N_o \left[1 - \frac{g_o N_p}{g_p N_o}\right]\mathcal{L}(\omega) = F\ \left[C_2 f_{op} N_o \mathcal{L}(\omega)\right], \tag{4}$$

where $\mathcal{L}(\omega)$ is the line shape and f_{op} is the absorption oscillator strength. From these expressions it is easy to determine that, to first order in $\kappa_{op}L$, equation (1) is obtained, with the widely cited corollary that two lines originating in the same upper level will always maintain the same ratio, a fact that is usually applied for the measurement of concentrations even though it can be easily violated in the experiments.

Calling $x \equiv \kappa_{op}L$, $y \equiv \kappa_{uv}L$ and defining $C_T \equiv y/x = \kappa_{uv}/\kappa_{op}$, under validity of equation (2) and introducing two auxiliary functions, namely:

$$G(\alpha, \beta) = \frac{[\alpha_{vu}\exp(\beta_{vu}) - 1]}{[\alpha_{po}\exp(\beta_{po}) - 1]} \tag{5}$$

and

$$P(C_T, x) \equiv \frac{[1 - \exp(-x)]}{[1 - \exp(-C_T x)]} \tag{6}$$

it follows that

$$\begin{aligned} C_T &= \frac{g_v f_{vu}}{g_p f_{po}} \frac{\alpha_{po}}{\alpha_{uo}\alpha_{vu}} G(\alpha,\beta)\exp(-\beta_{vp}) \\ &\equiv \frac{g_v f_{vu}}{g_p f_{po}} \alpha_{pv} G(\alpha,\beta)\exp(-\beta_{vp}). \end{aligned} \tag{7}$$

Then, the peak intensities ratio is given by our main result, namely:

$$R_I = \frac{I^{\mathrm{Peak}}_{po}}{I^{\mathrm{Peak}}_{vu}} = \frac{\omega^3_{po}}{\omega^3_{vu}} P(C_T, x) G(\alpha, \beta). \tag{8}$$

Taking into account equation (1), the general expression (8) should be compared with that for the ideal condition. Thus, the quotient:

$$Q = \frac{P(C_T, x) G(\alpha,\beta)}{\frac{g_p f_{po} \Gamma_{vu}}{g_v f_{vu} \Gamma_{po}} \exp(\beta_{vp})} \tag{9}$$

gives values near to unity for conditions close to LTE and optical thinness. On the contrary, departure from one or both of these ideal conditions are evidenced by Q different from unity.

Besides, it is interesting to note that C_T can take positive as well as negative values in conditions when κ_{uv} or κ_{op} are negative (zone of population inversion).

2.1 General properties and some useful approximations

From equation (8) we see that the variation of the intensities ratio depends basically on both functions $P(C_T, x)$ and $G(\alpha, \beta)$. Particular cases for equilibrium and/or thin sources situations can be easily derived. Of special interest are the first order expansions of $P(C_T, x)$; so

$$P(C_T, x \ll 1) = \frac{1}{C_T}, \tag{10}$$

$$N_n = \frac{N_\mathrm{e}\sum_{k<n} N_k \mathcal{E}_{kn} + N_\mathrm{e}\sum_{j>n} N_j \mathcal{D}_{jn} + \sum_{j>n} N_j A_{jn} + N_\mathrm{e} N_{(+)}(\mathcal{R}_n^{(2)} + N_\mathrm{e}\mathcal{R}_n^{(3)})}{N_\mathrm{e}\left[\sum_{k<n}\mathcal{D}_{nk} + \sum_{j>n}\mathcal{E}_{nj} + \mathcal{I}_n\right] + \sum_{k<n} A_{nk}}, \tag{15}$$

whereas

$$P(C_T \ll 1, x) \approx \frac{(1-\mathrm{e}^{-x})}{C_T x} \equiv P^{(1)}(C_T, x). \tag{11}$$

From equation (8), for thin sources and taking into account equation (10),

$$R_I^{\mathrm{thin}} = \frac{\omega_{po}^3}{\omega_{vu}^3}\frac{G(\alpha,\beta)}{C_T} = \left(\frac{\omega_{po}}{\omega_{vu}}\right)^3 \frac{g_p f_{po}}{g_v f_{vu}}\mathrm{e}^{\beta vp}, \tag{12}$$

which coincides with equation (1), as it must be expected. On the other hand, the case for thick sources (black body limit) is recovered noting that

$$P(C_T, x \gg 1) = 1$$

and

$$R_I^{\mathrm{thick}} = \frac{I_{po}^{\mathrm{Peak}}}{I_{vu}^{\mathrm{Peak}}} = \left(\frac{\omega_{po}}{\omega_{vu}}\right)^3 \frac{\mathrm{e}^{\beta vu}-1}{\mathrm{e}^{\beta po}-1}.$$

3 The four levels model

The proposed model consists of a total of four levels: the lower level l (which is going to be taken as the fundamental one, $l \equiv 0$), two excited levels n, k and the ionization limit I. A transition $n \to k$ is assumed to exist always, and we are going to consider two possible cases: case I which represents a "cascade" situation and so, besides $n \to k$, exists a transition $k \to l$ and case II where two lines, $n \to k$ and $n \to l$, share the same upper level. It should be noted that notation has been changed with respect to the more general treatment of Section 2, where an arbitrary number of levels could be considered. The levels labeled here l, n, k, and I are particular cases of the general model. The correspondence between the two different levels assignments is illustrated in Figure 1 together with sketches of the two cases.

Population distributions will be studied using the Collisional Radiative Steady State (CRSS) model. This model is a generalization of the models LTE and Corona Equilibrium (CE), being these ones the limiting cases for high and low electron densities, respectively [2]. It is valid in time dependent processes when the plasma characteristic time $t_{\mathrm{pl}} = \min(n_i/(\partial n_i/\partial t), T/(\partial T/\partial t))$ is larger than the time scale of atomic processes, that is $t_{\mathrm{pl}} \gg \tau_a = 1/n_e\langle v\sigma\rangle$.

There are seven dominating mechanisms that contribute to the population and de-population of the levels: spontaneous emission, electron impact ionization, three body recombination, electron impact excitation and de-excitation, radiative recombination and dielectronic recombination. Given the levels $|n\rangle$ and $|k\rangle$ and, provided

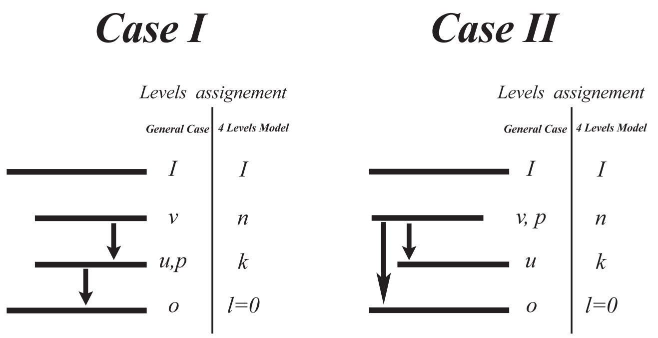

Fig. 1. Schematic representation of the proposed four-levels model showing both cases considered in this work and the reassignment of levels accordingly with Section 2.

that $E_n > E_k$, the excitation ($\mathcal{E}_{kn}$) and de-excitation ($\mathcal{D}_{nk}$) rates are related by:

$$g_k \mathcal{E}_{kn} = g_n \mathcal{D}_{nk} \mathrm{e}^{-\Delta E_{nk}/\Theta}, \tag{13}$$

where $\Delta E_{nk} \equiv E_n - E_k$.

On the other side, for a given generic level $|n\rangle$ (belonging to the ionization stage z), the ionization ($\mathcal{I}_n$) and three body recombination rates ($\mathcal{R}_n^{(3)}$) are related by the well known Saha equation [1]:

$$\mathcal{I}_n = 2\frac{g_{z+1}}{g_z}\left(\frac{m\Theta}{2\pi\hbar^2}\right)^{3/2} \mathrm{e}^{-(I_z - E_n)/\Theta}\mathcal{R}_n^{(3)} \equiv S(\Theta)\mathcal{R}_n^{(3)}. \tag{14}$$

In the above equation the factors g_z and g_{z+1} are the electronic partition functions for two ions of consecutive ionization degree. Considering all these processes and when steady state is achieved, that is when the population and de-population rates for a given level are equal, the population of a generic level $|n\rangle$ of ion z can be expressed by:

see equation (15) above

which leads to a system of coupled equations. In the above expression, $\mathcal{R}_n^{(2)}$ is the two-body recombination rate (radiative + dielectronic) while $N_{(+)}$ denotes the population of the ion $z+1$.

Defining

$$\mathcal{R}_n^{(2)} = \alpha_n^{\mathrm{R}} + \alpha_n^{\mathrm{D}}, \qquad \alpha_{nk} \equiv 1 + \frac{A_{nk}}{N_\mathrm{e}\mathcal{D}_{nk}},$$

$$\alpha_{n0} \equiv 1 + \frac{A_{n0}}{N_\mathrm{e}\mathcal{D}_{n0}}$$

and

$$\alpha_{nk}^* \equiv \alpha_{nk}\left(1 + \frac{\mathcal{D}_{n0}\alpha_{n0} + \mathcal{I}_n}{\mathcal{D}_{nk}\alpha_{nk}}\right)$$

the ratio N_n/N_k in our model of two excited levels n, k is given by:

$$\frac{N_n}{N_k} = \frac{\mathcal{E}_{kn}\left\{\left[1+\frac{N_0}{N_k}\frac{\mathcal{E}_{0n}}{\mathcal{E}_{kn}}\right]+\frac{N_{(+)}}{N_k}\frac{\mathcal{R}_n^{(2)}+N_e\mathcal{R}_n^{(3)}}{\mathcal{E}_{kn}}\right\}}{\mathcal{D}_{nk}\alpha^*_{nk}}.$$

In this way, if α^{**}_{nk} is defined as

$$\alpha^{**}_{nk} \equiv \frac{\alpha^*_{nk}}{\left[1+\frac{N_0}{N_k}\frac{\mathcal{E}_{0n}}{\mathcal{E}_{kn}}\right]+\frac{N_{(+)}}{N_k}\frac{\mathcal{R}_n^{(2)}+N_e\mathcal{R}_n^{(3)}}{\mathcal{E}_{kn}}}$$

and accordingly with equation (13), it follows that

$$\frac{N_n}{N_k} = \frac{(N_n/N_k)_{\rm eq}}{\alpha^{**}_{nk}}. \qquad (16)$$

Up to this point no approximations have been made. To evaluate (16), N_0/N_k and $N_{(+)}/N_k$ have to be estimated.

Operating in an analogous form as for N_n/N_k and using the notation:

$$\alpha_{k0} = 1+\frac{A_{k0}}{N_e\mathcal{D}_{k0}}, \qquad \alpha^*_{k0} \equiv \alpha_{k0}\left(1+\frac{\mathcal{E}_{kn}+\mathcal{I}_n}{\mathcal{D}_{k0}\alpha_{k0}}\right)$$

and

$$\alpha^{**}_{k0} = \frac{\alpha^*_{k0}}{\left[1+\frac{N_n\mathcal{D}_{nk}\alpha_{nk}+N_{(+)}\left(\mathcal{R}_k^{(2)}+N_e\mathcal{R}_k^{(3)}\right)}{N_0\mathcal{E}_{0k}}\right]},$$

the ratio N_0/N_k is given by:

$$\frac{N_0}{N_k} = \alpha^{**}_{k0}\,(N_0/N_k)_{\rm eq}. \qquad (17)$$

For obtaining $N_{(+)}/N_k$ we consider that

$$N_{(+)}/N_k = \frac{N_{(+)}/N_0}{N_k/N_0} = \frac{\frac{\mathcal{I}_0}{(\mathcal{R}_0^{(2)}+N_e\mathcal{R}_0^{(3)})}}{\frac{(N_k/N_0)_{\rm eq}}{\alpha^{**}_{k0}}}.$$

Finally, N_n/N_0 must be evaluated. Clearly, if the complete terms are written, the resulting equations cannot be uncoupled. Therefore we make here the unique approximation in our model for calculating N_n/N_0, namely to consider that we have a two levels system disregarding the de-excitation $n \to k$. Thus, defining

$$\alpha^*_{n0} \equiv \alpha_{n0}\left(1+\frac{\mathcal{I}_n}{\mathcal{D}_{n0}\alpha_{n0}}\right); \qquad \alpha^{**}_{n0} = \frac{\alpha^*_{n0}}{1+\mathcal{I}_n/\mathcal{E}_{0n}}$$

results

$$\frac{N_n}{N_0} = \frac{(N_n/N_0)_{\rm eq}}{\alpha^{**}_{00}}, \qquad (18)$$

being the above equation the only approximated expression of the model. Its validity is proved since N_n/N_k results:

$$\frac{N_n}{N_k} = \frac{N_n}{N_0}\frac{N_0}{N_k}(\pm 3\%).$$

In summary, we have shown that in the proposed model, the populations ratio for any pair of levels can always be written in terms of the general form of equation (2).

4 Rate equations

In order to calculate the different α coefficients we need data about the involved rate coefficients which general expression is related with the cross-section $\sigma(E)$ and the electron speed v through:

$$\text{Rate} = \int_{\Delta E}^{\infty} v\sigma(E)F(E)\mathrm{d}E.$$

Here ΔE is the threshold energy of the process and $F(E)$ is the energy distribution function. Due to the cumbersome nature of *ab initio* calculations of cross-sections it is imperative to use some sort of semi-empirical approximations in order to arrive to manageable expressions.

In this section, we summarize the formulae employed in the calculations of our model. For radiative and dielectronic recombinations we will use the formulae given, in terms of adjustable parameters, in the book by Sobelman *et al.* [13].

4.1 Transition probabilities

The values for the A_{nk} (or $f_{nk} \equiv 1.5A_{nk}\sigma^{-2}$, being σ the wave number measured in cm^{-1}) can be obtained from experimental data or, if these are unknown, from theoretical calculations using the approach Multi-Configurations Hartree Fock (MCHF) [15]. In our case, both points of view have been used, taking into account that for strong transitions both values are in good agreement. The results were, in practice, independent of this choice. Typical values for strong lines of neutral atoms are: $f_{nk} = 0.4$, $\sigma = 20\,000$ cm^{-1} and $A_{nk} \approx 10^8$ s^{-1}. For ionized atoms and for a similar value of f_{nk} results $A_{nk} \propto Z^4$.

4.2 Electron impact excitation and de-excitation

A general expression for the rate $\mathcal{E}_{kn}$ useful for both, allowed ($f_{nk} \neq 0$) and forbidden transitions ($f_{nk} = 0$) was formulated by Sobelman *et al.* [13]. In this case

$$\mathcal{E}_{kn} \propto \sum_K Q_K(k,n)G_K(\beta); \qquad \beta \equiv \Delta E/\Theta$$

being $Q_K(k,n)$ the angular factors and $G_K(\beta)$ a set of functions tabulated in the book from Sobelman. The summation index, K (arising from the multipole expansion), takes values related with the orbital quantum numbers: $K = |l_k - l_n| \ldots |l_k + l_n|$.

Typical values for optically allowed lines with transition energy ΔE can be estimated using the van Regemorter formula [13]:

$$\mathcal{E}_{kn} \simeq 6.4 f_{kn}\times 10^{-8}\left(\frac{Ry}{\Delta E}\right)^{3/2}\beta^{1/2}\mathrm{e}^{-\beta}\left[\mathrm{cm^3 s^{-1}}\right],$$

where $Ry \equiv 13.6$ eV. For a transition with $\Delta E \approx 2.5$ eV, $f_{kn} \approx 0.4$ and $\beta \approx 1$, results $\mathcal{E}_{kn} \approx 1.2 \times 10^{-7}$ $\mathrm{cm^3\,s^{-1}}$.

4.3 Electron impact ionization and recombination

The ionization of a shell containing m electrons, denoted by $n_0 l_0^m$ can be estimated from the widely used formula due to Lotz [2,13]:

$$\mathcal{I}_0 = 4.3m \times 10^{-8} \left(\frac{Ry}{I}\right)^{3/2} \beta^{1/2} \left(-\mathrm{Ei}(-\beta)\right) \left[\mathrm{cm}^3\mathrm{s}^{-1}\right]$$
$$\beta \equiv E_z/\Theta, \tag{19}$$

where $Ry \equiv 13.6$ eV, I is the ionization limit and Ei indicates the exponential integral. Thus, typical values for neutral atoms with ionization energies in the order of 13 eV and for $kT \approx 2.5$ eV are $\mathcal{I}_0 \approx 10^{-10}$ cm^3 s^{-1}. The approximate scaling with the ionization order z is given by $\mathcal{I}_z = \mathcal{I}_0/z^3$.

5 Considerations about the escape factors

For an optically thin and homogeneous plasma, the source conditions can be taken as invariant during the time it takes light to travel across it. However, for optically thick plasmas, the light undergoes several processes, such as scattering, absorption and re-emission, before escaping. An "escape factor" is defined for taking into account these processes and to relate them with the thickness of the source:

$$\chi_{op}(\kappa_{op}L) = \int_{-\infty}^{\infty} \mathrm{e}^{-\kappa_{op}(\omega)L}\mathcal{L}(\omega)\mathrm{d}\omega, \tag{20}$$

where $\mathcal{L}(\omega)$ is the line shape. A classical treatment of escape factors is due to Holstein [1] and a plot of its value as a function of the source thickness can be found in reference [16] for the case of a Doppler broadened line. However, this approach assumes that collisional processes (excitation and de-excitation) are negligible and thus do not take place in modifying the levels populations [1]. Asymptotic values of $\chi_{op}(\kappa_{op}L)$ are: $[\kappa_{op}L(\pi\ln(\kappa_{op}L))^{1/2}]^{-1}$ for Gaussian line shapes and $(\pi\kappa_{op}L)^{-1/2}$ for Lorentzian ones. When the source is thin, the escape factor is ≈ 1.

More recently, Netzer [17] evaluated equation (20) using numerical methods and found that, within a factor ≤ 3, $\chi_{op}(\kappa_{op}L)$ can be fitted by the expression:

$$\chi_{op}^{\mathrm{Netzer}}(\kappa_{op}L) \approx \frac{1-\exp(-\kappa_{op}L)}{\kappa_{op}L}$$

that is equal to $(1-\mathrm{e}^{-x})/x$ in our notation (see Sect. 2).

On the other hand, as seen from equation (8), the intensities ratio is a function of two variables. Thus, conditions close to ideality arise when both x and C_T are small enough. The approximation (11) of equation (6),

$$P^{(1)}(C_T, x) = \frac{1-\mathrm{e}^{-x}}{C_T\, x},$$

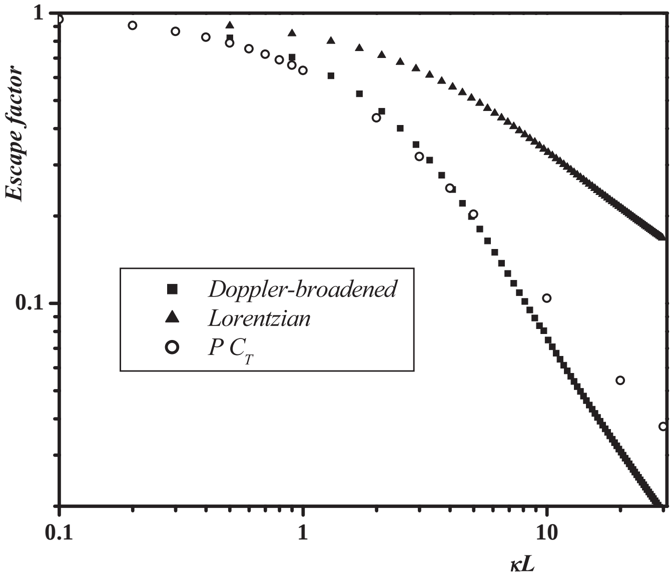

Fig. 2. Escape factors as a function of the (dimensionless) source thickness, κL, for a Doppler-broadened line (squares), and Lorentzian line (triangles) compared with the product $C_T P(C_T, x)$ (open circles).

is verified when the quotient $C_T = y/x \equiv \kappa_{uv}L/\kappa_{op}L \ll 1$ (irrespective of their individual values). Thus, it is possible to identify:

$$\chi_{op}^{\mathrm{Netzer}}(\kappa_{op}L) \approx C_T P^{(1)}(C_T, x).$$

Considering the fact that (i) as mentioned above, the classical approach neglects collisional effects while our function $C_T P(C_T, x)$ takes into account both, radiative and collisional processes, and (ii) as shown in Figure 2, the curve resulting from it lies between the Gaussian and Lorentzian limits, it is reasonable to propose

$$\chi_{op}(\kappa_{op}L) = C_T P(C_T, x) \tag{21}$$

as a good approximation for describing escape factors, regardless of the relative importance between collisional and radiative processes.

6 Results

Equation (8) summarizes the main result of the present work in terms of the product:

$$P(C_T, x)G(\alpha, \beta) = \frac{I_{po}^{\mathrm{Peak}}}{I_{vu}^{\mathrm{Peak}}} \frac{\omega_{vu}^3}{\omega_{po}^3},$$

since it basically represents the peak intensities ratio as a function of the parameters N_e, T. Additionally we have also obtained the absorption coefficients in terms of equation (4) and thus the regions where population inversion is possible. As stated in Section 3 two cases were considered: case I, where the existing transitions are $n \to k, k \to 0$ and case II for transitions with the same upper level, that is: $n \to k, n \to 0$.

Case I corresponds *e.g.*, to transitions of the type $6p \to (5d + 6s)$, $(5d + 6s) \to 5p^n$ in noble gases presenting several grades of ionization, such as Xe^+ and Xe^{3+}. Case II is found, for example, for transitions $3s$–$3p$ (5 801 and 5 812 Å) and $2s$–$3p$ (312 Å) belonging to the ion C^{3+} and also in Xe^+ for lines with $\lambda = 4\,844$ Å and $\lambda = 5\,460$ Å corresponding to transitions $6s$–$6p$.

For both cases the electronic temperature T and the electronic density of the plasma N_e, were used as parameters. Typical ranges for them were: 10^{14} cm^{-3} $< N_e < 10^{20}$ cm^{-3} and $I/20 < kT < I/7$. In all cases the lowering of the ionization level (ΔI) was taken into account accordingly with the equation mentioned in the book by Griem [1]. If energy is measured in eV, a_0 is the Bohr radius (5.3×10^{-9} cm), ρ_D is the Debye radius ($\approx 740\sqrt{kT/N_e}$) and Z_c is the spectroscopic symbol, then ΔI is taken as: $\Delta I = 27.2\,(Z_c - 1)\,a_0\rho_D$. To illustrate the model's behavior for different source thicknesses, the parameter $x = \kappa L$ (defined in terms of the absorption in Sect. 2) was set to different values. Even when the absorption κ is a function of the plasma conditions, and must be computed for each pair (N_e, kT) in terms of equation (4), there is still a free parameter, namely the source length, L, which can be used to control the source thickness. So, there is no loss of generality in considering x as a free parameter in the calculus.

For each case the quotient Q between the real intensities ratio of two lines, $P(C_T, x)G(\alpha, \beta)$, and the ideal intensities ratio (in the limits of optically thin source and LTE) were calculated as indicated in equation (9). They are a measurement of the degree of ideality (LTE and thin source) of the system for each pair (N_e, kT): $Q \sim 1$ indicates nearly ideal conditions.

Two practical uses of this formalism in our laboratory are: (i) the measurement of relative emission oscillator strengths (f_{ij}) deduced from the line intensities [21–23]:

$$\frac{g_p f_{po}}{g_v f_{vu}} = P(C_T, x)G(\alpha, \beta)\exp(\beta_{pv})\frac{\Gamma_{po}}{\Gamma_{uv}},$$

and (ii) knowing the f_{ij}, the determination of relative concentrations, of interest in applied spectroscopy. The first step in this process is the verification of the source thinness by comparison of the relative intensities of two lines arising from a common upper level. Using the formalism developed in this work, a 3 dimensional plot similar to our Figures 3a or 3b is obtained, from which the departure from ideal conditions can be deduced. Figure 3a corresponds to case I for an ideally thin source with $x = 10^{-4}$. Calculations were made using the ion parameters (energy levels, levels multiplicities, ionization potential, etc.) of Xe^+. For this ion, LTE is expected in the surface delimited by 10^{16} cm^{-3} $< N_e < 10^{18}$ cm^{-3} and 2 eV $< kT <$ 3 eV; in this zone $Q \sim 1$. For densities higher than 10^{18} cm^{-3}, and even in the case of a thin source, effects due to lowering of the ionization limit are important ($> 10\%$). In this region Q trends approximately to 0.6 instead of reaching the value of 1, as it should be expected on the basis of equilibrium considerations. However, some interesting applications such as LIBS are considered for $N_e \le 10^{18}$ cm^{-3}. For the sake of comparison the case of $x = 1$ can be seen in Figure 3b showing a similar behavior but with Q lowered due to the thickness of the source.

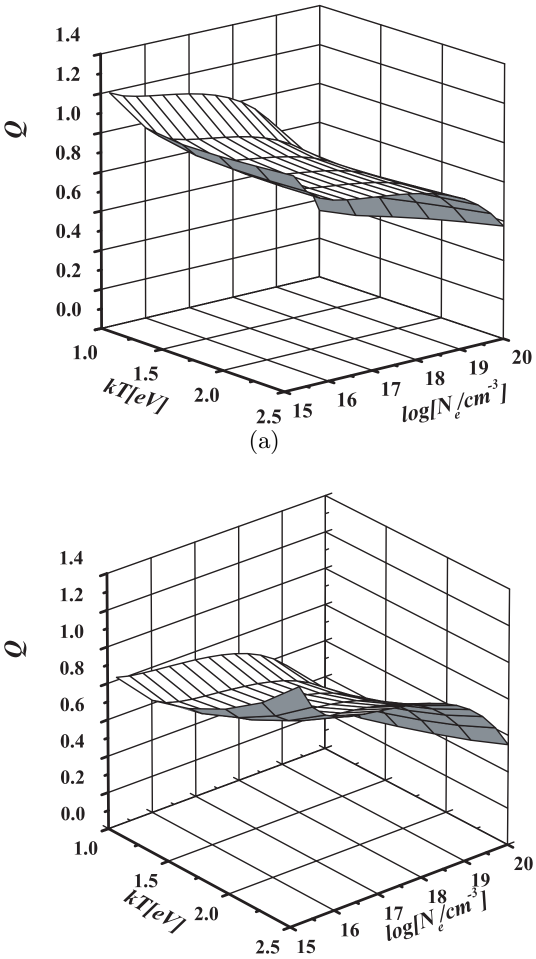

Fig. 3. (a) Plot of Q (case I), as defined in equation (9) for the ion Xe^+ and for a thin source ($x \equiv \kappa L = 10^{-4}$). (b) Plot of Q (case I), as defined in equation (9) for the ion Xe^+ and for a thick source ($x \equiv \kappa L = 1$).

Similar results were found for Xe^{2+} and Xe^{3+}. Of special interest for this last ion is the factor F introduced in equation (4), which is proportional to the absorption coefficient (κ_{nk}) between levels $|k\rangle$ and $|n\rangle$. In Figure 4 is shown, as contours levels, that F takes negative values in the region delimited by $N_e \lesssim 3 \times 10^{15}$ cm^{-3} and 2 eV $< kT <$ 4.25 eV. It is interesting to point out that for Xe^{3+}, and precisely in this region of the plane $N_e - kT$ (predicted by our model as a zone of negative absorption), was experimentally found by Papayoanou *et al.* [18] that population inversion occurs.

Concerning with case II, different situations can be found depending on the given ion. When $C_T \ll 1$ we can

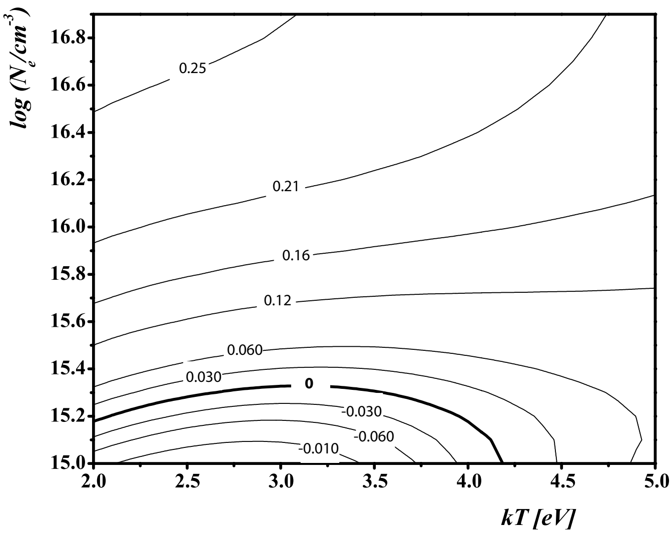

Fig. 4. Contour levels for the F factor defined in equation (4), showing the region of possible population inversion ($F < 0$) for Xe^{3+}.

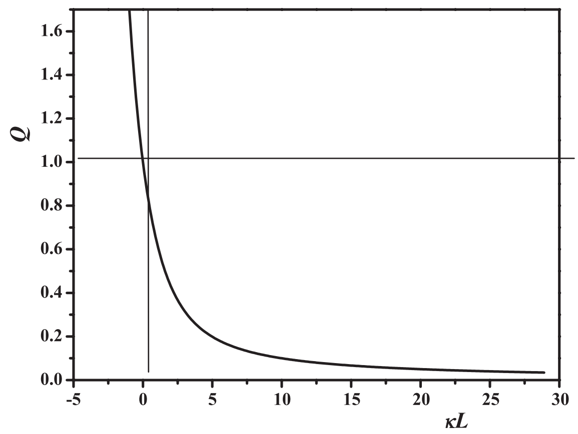

Fig. 5. Plot of the first order expansion of Q (case II), as defined in equation (22) for the ion C^{3+} and for $-1 \leq x \leq 30$.

use equations (11, 7) and our equation (9), such that

$$Q = \frac{1 - \mathrm{e}^{-x}}{x}, \tag{22}$$

irrespective of the particular x value. For increasing and positive values of x (proportional to the lower level population) we recover the result known as self-absorption. However, if $x < 0$ (for regions where population inversion occurs), then $Q > 1$ and

$$\frac{I_{nl}^{\text{Peak}}}{I_{nk}^{\text{Peak}}} > \left[\frac{I_{nl}^{\text{Peak}}}{I_{nk}^{\text{Peak}}}\right]_{\text{LTE}}.$$

As an example of this last situation, Xe^+ lines with $\lambda = 5\,419$ Å and $\lambda = 4\,890$ Å arising from level $(^3\text{P})6p[3]_{5/2}$ [20] can be considered where, effectively the line with $\lambda = 5\,419$ Å shows laser action. Please note that for this particular case the lower level is not the fundamental one. The behavior of equation (22) is shown in Figure 5.

7 Conclusions

The present work describes a Collisional Radiative Steady State model for a system of two excited levels (n, k with $E_n > E_k$), the ionization level I (with energy $E_I > E_n$) and the ground level l (with $E_l = 0$). Two different situations were considered. Case I, treating "cascade" transitions $n \to k$ and $k \to l$, found, *e.g.* in Xe^+ between levels $6p \to (6s, 5d) \to 0$. Case II which corresponds to transitions originating in the same upper level, that is $n \to k$, $n \to l$. The electronic temperature (T) and the electronic density of the plasma (N_e), were used as parameters. Both cases were treated in the optically thin and optically thick source limits and the lowering of the ionization limit was included.

Main conclusions of this work can be summarized as follows.

(1) The analysis of figures like 3 and 5 indicate the departure from ideal conditions.
(2) A good qualitative description for the escape factor is provided by our function $C_T P(C_T, x)$.
(3) For case I and even for a thin source ($x \ll 1$), the influence of the lowering can be noticed for increasing electron densities, precisely when LTE is expected to dominate accordingly with canonical assumptions (see Fig. 3a). For thicker sources, the general trend is similar but Q is always smaller, as shown in Figure 3b.
(4) Population inversion is predicted by the model for the same plasma conditions as those found experimentally by other authors (see Fig. 4).
(5) For case II and for $C_T \ll 1$ the quotient $I_{nl}^{\text{Peak}}/I_{nk}^{\text{Peak}}$ its smaller than its ideal value for positive and increasing x, which describes the so-called self-absorption. The possibility of a reverse situation was analyzed and included in Figure 5 by extending x to negative values (the gain region).
(6) The model could be used in plasmas containing more than one element as pollutant or traces and the ratio of them is of interest. In this case this is directly given by comparison of the coefficients α^{**} of both elements.
(7) From the property

$$P\,(C_T, x \to 0) = 1/C_T$$

it follows that a source can be considered as thin (up to a given percent) when the condition

$$P\,(C_T, x)\, C_T \approx 1$$

between the same percentage.

At present we are working in more complete model which takes into account a greater number of levels of the ion of interest as well as the previous and subsequent ionization stages.

References

1. H.R. Griem, *Principles of Plasma Spectroscopy* (Cambridge Univ. Press, Cambridge, 1997).
2. D. Salzmann, *Atomic Physics in Hot Plasmas* (Oxford Univ. Press, New York and Oxford, 1998).
3. D. Mihalas, *Stellar Atmospheres*, 2nd edn. (Freeman, San Francisco, 1978).
4. A.F. Molisch, B.P. Oehry, G. Magerl, J. Quant. Spectrosc. Radiat. Transfer **48**, 377 (1992).
5. A.F. Molisch, B.P. Oehry, W. Schupita, G. Magerl, Comput. Phys. Commun. **77**, 255 (1993).
6. G.J. Parker, W.N.G. Hitchon, J.E. Lawler, J. Phys. B **26**, 4643 (1993).
7. A.K. Kazansky, N.N. Bezuglov, J. Phys. B **33**, 99 (2000).
8. A.K. Kasansky, N.N. Bezuglov, F. Fuso, M. Allegrini, Phys. Rev. A **63**, 042703 (2001).
9. A.K. Kasansky, N.N. Bezuglov, A.F. Molisch, F. Fuso, M. Allegrini, Phys. Rev. A **64**, 022719 (2001).
10. M. Klapisch, A. Bar-Shalom, J. Orej, D. Colombant, Phys. Plasmas **8**, 1817 (2001).
11. *Laser Induced Plasmas and Applications*, edited by L.J. Radziemsky, D.A. Cremers (Marcel Dekker, New York and Basel, 1989).
12. G. Bertuccelli, H.O. Di Rocco, J. Quant. Spectrosc. Radiat. Transfer **55**, 463 (1996).
13. I.I. Sobelman, L.A. Vainshtein, E.A. Yukov, *Excitation of Atoms and Broadening of Spectral Lines* (Springer, Berlin, 1981).
14. A. Corney, *Atomic and Laser Spectroscopy* (Clarendon Press, Oxford, 1977).
15. R.D. Cowan, *The Theory of Atomic Structure and Spectra* (University of California Press, Berkeley and Los Angeles, 1981).
16. H. Zwicker, "Evaluation of Plasma Parameters in Optically Thick Plasmas", in *Plasma Diagnostics,* edited by W. Lochte-Holtgreven (North-Holland Publishing Company, Amsterdan and John Wiley & Sons Inc, New York, 1968).
17. H. Netzer, *The formation of FeII emission Lines*, in *Physics of Formation of FeII Lines Outside LTE*, edited by R. Viotti *et al.* (Reidelo Publishing Company, 1988).
18. A. Papayoanou, R.G. Buser, I.M. Gumeiner, IEEE J. Quant. Electron. **QE-9**, 580 (1973).
19. W. Lochte-Holtgreven, Evaluation of Plasma Parameters, in *Plasma Diagnostics,* edited by W. Lochte-Holtgreven (North-Holland Publishing Company, Amsterdan and John Wiley & Sons Inc, New York, 1968).
20. J.E. Hansen, W. Persson, Phys. Scripta **36**, 602 (1987).
21. H.O. Di Rocco, D.I. Iriarte, J.A. Pomarico, Eur. Phys. J. D **10**, 19 (2000).
22. G. Bertuccelli, H.O. Di Rocco, D.I. Iriarte, J.A. Pomarico, Phys. Scripta **62**, 277 (2000).
23. D.I. Iriarte, M. Romeo y Bidegain, G. Bertuccelli, H. Di Rocco, Phys. Scripta **57**, 495 (1998).